

“Anomalous” Optical GRB Afterglows are Common: Two $z \sim 4$ Bursts, GRB 060206 and 060210¹

K. Z. Stanek², X. Dai², J. L. Prieto², D. An², P. M. Garnavich³, M. L. Calkins⁴, J. Serven⁵,
G. Worthey⁵, H. Hao⁶, A. Dobrzycki⁷, C. Howk³, T. Matheson⁸

kstanek@astronomy.ohio-state.edu

ABSTRACT

We report on two recent $z \sim 4$ gamma-ray bursts (GRBs), GRB 060206 and GRB 060210, for which we have obtained well-sampled optical light curves. Our data, combined with early optical data reported in the literature, shows unusual behavior for both afterglows. In R -band GRB 060206 ($z = 4.045$) experienced a slow early decay, followed by a rapid increase in brightness by factor ~ 2.5 about 1 hour after the burst. Its afterglow then faded in a broken power-law fashion, with a smooth break at $t_b = 0.6$ days, but with additional, less dramatic ($\sim 10\%$) “bumps and wiggles”, well detected in the densely sampled light curve. The R -band afterglow of GRB 060210 ($z = 3.91$) is also unusual: the light curve was more or less flat between 60 and 300 sec after the burst, followed by $\sim 70\%$ increase at ~ 600 sec after the burst, after which the light curve declined as a $\sim t^{-1.3}$ power-law. Despite reports to the contrary, we find that for GRB 060206 X-rays follow the optical decay, but with significant variations on short timescales. However, the X-ray afterglow is contaminated by a nearby, variable source, which especially at late times obscures the behavior of the X-ray afterglow. The early X-ray light curve of GRB 060210 exhibited two sharp flares, without corresponding peaks in the optical light. We find that the late X-ray light curve is well described

¹Based on data from the MDM 2.4-m and 1.3-m telescopes

²Dept. of Astronomy, The Ohio State University, Columbus, OH 43210

³Dept. of Physics, University of Notre Dame, Notre Dame, IN 46556

⁴F. L. Whipple Observatory, Amado, AZ 85645

⁵Dept. of Physics, Washington State University, Pullman, WA 99164

⁶Harvard-Smithsonian Center for Astrophysics, Cambridge, MA 02138

⁷European Southern Observatory, Garching bei München, Germany

⁸NOAO Gemini Science Center, Tucson, AZ 85719

by a broken power-law model, with a smooth break at ~ 8 hours after the burst. The early decay index of the X-ray light curve is not consistent with the $\sim t^{-1.3}$ power-law seen in optical.

We argue that “anomalous” optical afterglows are likely to be the norm, and that the rapid variations often seen in *Swift*-XRT data would also be seen in the optical light curves, given good enough sampling. As a result, some of the often employed procedures, such as deriving the jet opening angle using a broken power-law fit to the optical light curves, in many cases might have a poor statistical significance. Finally, we argue that the rapid rise at ~ 3000 sec in the optical for GRB 060206 and the optical bump at ~ 700 sec in GRB 060210 might be due to the turn-on of the external shock. If indeed the case, the existence and timing of such features could provide valuable additional information about the energy of the GRB jet and the density of the circumburst medium it is plowing into.

Subject headings: gamma-rays: bursts

1. Introduction

Gamma-ray bursts (GRBs) continue to surprise us. With the *Swift* satellite (Gehrels et al. 2004) providing quick and accurate localizations for many bursts (for example, 20 GRBs were localized between January 1st - February 15th, 2006), it is now possible to find and study in even more detail bursts which are “unusual”. Those are more than just mere curiosity—they test and verify our understanding of physics of these extreme events.

The physics of GRB afterglow emission appears on solid footing. The GRB sweeps up ambient gas and the resulting shock emits synchrotron radiation from X-rays to radio wavelengths (e.g. Piran 2005). The light curve decays as a power-law with a break when the opening angle of the beamed emission exceeds the opening angle of the jet (e.g., Stanek et al. 1999; Rhoads 1999). But the fast localizations of the *Swift* satellite means that optical and X-ray observations can begin before the γ -rays have completely faded. The transition between the end of the “prompt” emission and the rise of the shocked ambient gas emission is uncertain territory. Internal shocks may be the source of prompt emission or continued activity from the central engine may inject more energy into the external shock. Deciphering the effects of these processes requires high-quality observations obtained rapidly after the burst. What also helps is time dilation. High-redshift bursts have the advantage of being observed in slow motion.

Two such high-redshift bursts have been recently detected by the *Swift* satellite. GRB 060206 triggered *Swift*-BAT on Feb. 6, 04:46:53 UT (Morris et al. 2006a). A likely afterglow has been identified by Fynbo et al. (2006a), who also determined that the afterglow was at high redshift of $z = 4.045$ (Fynbo et al. 2006b). A presence of a bright afterglow has been reported by several groups, most notably by RAPTOR (Wozniak et al. 2006a), who indicated that the afterglow has increased in brightness by ~ 1 mag about 1 hour after the burst. Wozniak et al. (2006b) has released detailed description of the RAPTOR data for this event, which we will discuss later in this paper.

GRB 060210 triggered *Swift*-BAT on Feb. 10, 04:58:50 UT (Beardmore et al. 2006a). Fox & Cenko (2006) have quickly identified a possible afterglow, and Cucchiara et al. (2006) measured a high redshift of $z = 3.91$. KAIT robotic telescope has obtained extensive optical observations starting as soon as 62 sec after the burst (Li 2006a), indicating that the afterglow brightened by 0.4 mag by 9 minutes after the burst (Li 2006b). Beardmore et al. (2006b) reported on the *Swift*-XRT data, which showed two strong flares 200 sec and 385 sec after the trigger, followed by a power-law decay.

In this paper we report on our optical follow-up of these two bursts. Our data, described in Section 2, combined with the data reported in the literature clearly shows two very unusual optical afterglows, whose evolution we describe in Section 3. In section 4 we analyze *Swift*-XRT data for these two events. We briefly summarize our results and discuss their implications in Section 5.

2. The Optical and X-Ray Data

The majority of our data were obtained with the MDM-2.4m telescope, with additional data obtained using the MDM-1.3m telescope. For the bright afterglow of GRB 060206, we have obtained 83 high signal-to-noise *R*-band images between 1.7 and 8.7 hours after the burst, followed by additional 16 *R*-band images during the next two nights. For the much fainter afterglow of GRB 060210, we have obtained 12 *R*-band images between 0.48 and 2.0 hours after the burst, until the object has set.

All the light curves were extracted using ISIS2 image subtraction package (Alard 2000). To obtain absolute calibration, for GRB 060206 we used nine stars in the field with SDSS photometry (Cool et al. 2006; Adelman-McCarthy et al. 2006) to transform to the standard system fitting a zero-point difference and a color-term. We used the transformation equations of Lupton (2005) to transform SDSS *griz* magnitudes to BVRI. For future references and cross-calibrations, this transformation gives $R = 15.89 \pm 0.02$ mag and $I = 15.47 \pm 0.02$ mag

for the star SDSS J133130.4+350416.1. We assumed $R - I \simeq 0.6$ mag for the afterglow (Greco et al. 2006). The absolute photometric calibration is thought to be better than $\sim 5\%$. We found that in order to match Wozniak et al. (2006b) data to our data, we had to subtract 0.22 mag from their unfiltered R -band magnitudes (see Fig.2). This offset does not affect any of our conclusions. For GRB 060210 we used the calibration of the field obtained with the KAIT telescope (Li et al. 2006, in preparation). A USNO-B1 (Monet et al. 1998) star 1170-0048923 at RA = 03:50:53.00, DEC = +27:01:30.54 (J2000), which is close to the GRB, is measured at $R = 15.64$ mag using KAIT calibration, 0.29 mag fainter than the USNO magnitude. This is not unusual, since the magnitudes of stars in the USNO-B1 catalog were obtained with photographic plates. Tables 1 and 2 present our R -band photometry for the two bursts.

We have also analyzed the X-ray data obtained by the *Swift*-XRT instrument. We started with the XRT level 2 event files for both the windowed timing mode and the photon counting mode observations. There was a hot CCD column in the windowed timing observation for GRB 060206. We filtered the events on these hot CCD pixels. We used the `xselect`¹ software package to extract the X-ray light curves and spectra. The background subtracted light curves were adaptively binned according to the signal-to-noise ratios. We fit the spectra with `XSPEC` (Arnaud 1996) to convert XRT count rates to fluxes. We use the `rmf` files from standard XRT calibration distribution, and generated the `arf` files with the *Swift*-XRT software tool `xrtmkarf`².

3. Evolution of Optical Afterglows

Figure 1 presents the R -band light curves for GRB 060206 and GRB 060210 (see Tables 1,2). In addition to our MDM 2.4-m data, we have added some data from the literature to extend the time coverage. For GRB 060206, we add one early data point from Guidorzi et al. (2006) and 101 densely sampled RAPTOR data points from Wozniak et al. (2006b). For GRB 060210, we add eight very early data points from the KAIT telescope reported by Li (2006a,b). All the literature data were brought to the common zero-point with our data, using overlaps between the data sets.

Figure 1 shows most unusual behavior for both afterglows. As described in detail by Wozniak et al. (2006b), GRB 060206 experienced a slow early decay, followed by a rapid

¹<http://heasarc.gsfc.nasa.gov/docs/software/lheasoft/ftools/xselect/xselect.html>

²http://swift.gsfc.nasa.gov/docs/swift/analysis/xrt_swguide_v1.2.pdf

increase in brightness by ~ 1 mag about 1 hour after the burst. Its afterglow then faded in a typical broken power-law fashion, with a smooth break at $t_b = 0.6$ days, but with additional, less dramatic ($\sim 10\%$) “bumps and wiggles”, well detected in the densely sampled light curves. These deviations from smooth decay can be seen better in Figure 2, where we show the RAPTOR data and our first night MDM data.

To characterize the long timescales behavior of its afterglow, we have fit all our GRB 060206 R -band data with the broken power-law model of Beuermann et al. (1999) (see also Stanek et al. 2001):

$$F_R(t) = \frac{2F_{R,0}}{\left[\left(\frac{t}{t_b}\right)^{\alpha_1 s} + \left(\frac{t}{t_b}\right)^{\alpha_2 s}\right]^{1/s}}, \quad (1)$$

where t_b is the time of the break, $F_{R,0}$ is the R -band flux at t_b and s is a parameter which determines the sharpness of the break, where a larger s gives a sharper break. This formula smoothly connects the early time $t^{-\alpha_1}$ decay ($t \ll t_b$) with the later time $t^{-\alpha_2}$ decay ($t \gg t_b$). The fit results in the following values for the parameters: $\alpha_1 = 0.7, \alpha_2 = 2.0, t_b = 0.6$ days. Given that the data show clear variations from the smooth behavior, these are only approximate values, and should be treated with caution (see the Discussion below). The overall fit is reasonable and it supports a break in the light curve, traditionally interpreted as a jet break (e.g. Stanek et al. 1999). This is broadly consistent with the behavior in other optical bands reported by LaCluyze et al. (2006) and Reichart et al. (2006).

The R -band afterglow of GRB 060210 ($z = 3.91$) closely resembles recently reported behavior of GRB 0508101 (Rykoff et al. 2006), who called that event an “Anomalous Early Afterglow”. The light curve of GRB 060210, as reported by Li (2006b), was more or less flat between 60 and 300 sec after the burst, followed by ~ 0.4 mag increase by ~ 600 sec after the burst. Using Li (2006b) and our data we show that the light curve then declined as a $\sim t^{-1.3}$ power-law. If we bring GRB 060210 to a fiducial redshift of $z = 1$, which is close to a likely redshift of GRB 050801 (Rykoff et al. 2006), then these two burst are even closer in their evolution, as can be seen comparing to their Figure 1.

4. Comparison of Optical to X-Ray Data

Given the unusual behavior observed in the optical wavelengths for these two bursts, it is useful to investigate their X-ray light curves as well. Indeed, X-ray afterglows observed by *Swift*-XRT have been shown to have features (Nousek et al. 2006) not expected in the standard afterglow models, including giant flares such as observed in GRB 050502B (Falcone et al. 2006). The origin of the flares is still under investigation (e.g. Zhang et al.

2006; Perna et al. 2005).

In Figure 3 we compare the X-ray to optical light curves for GRB 060206. While it was intrinsically a very bright afterglow in optical, it was a faint X-ray event, with the ratio of $F_{\nu,R}/F_{\nu,X} \sim 1000$. Despite earlier reports to the contrary (Morris et al. 2006b), the overall behavior between the two bands is similar, but with clear short-timescale variations, as reported before by Morris et al. (2006b). However, by analyzing the later XRT observation, we clearly see a nearby, contaminating X-ray source, about $15''$ away. This nearby source is most likely variable, obscuring the true behavior of the X-ray afterglow, especially at later times. That also explains the flattening of the late X-ray light curve, as seen in Figure 3.

In Figure 4 we compare the X-ray to optical light curves for GRB 060210. Here the ratio of $F_{\nu,R}/F_{\nu,X} \sim 10$, much lower than for GRB 060206. As reported by Beardmore et al. (2006b), X-rays show two strong flares 200 sec and 385 sec after the trigger, followed by a smoother decay. As already reported by Dai & Stanek (2006), the analysis of the entire XRT light curve indicates a presence of a broken power-law. They fitted both a single power-law and a broken power-law model to the XRT light curve from 3.0×10^3 sec to 1.0×10^6 sec after the BAT trigger. For the single power-law model they found a decay index of $\alpha = 1.09$, but the fit was poor. For the broken power-law model they found $\alpha_1 = 0.7, \alpha_2 = 1.4, t_b = 7.9$ hours, with the broken power-law providing a much better fit. The power-law decay index for the X-ray light curve before the jet break is not consistent with the optical decay index of ~ 1.3 discussed above. It would be most interesting to add later R -band data for this event to see if the X-rays are indeed different from optical.

We note that the X-ray flares in GRB 060210 do not have corresponding optical peaks (as far as we can tell from the data reported by Li 2006b). This would indicate that the X-ray flares are occurring in a different region from where the optical light is formed.

5. Summary and Discussion

We have presented optical light curves for two recent $z \sim 4$ afterglows, GRB 060206 and GRB 060210. They both show unusual behavior, with significant re-brightening by as much as factor of ~ 2.5 about 1 hour (~ 10 min in the rest frame) after the burst in case of 060206. GRB 060210 also shows unusual optical evolution, similar to “anomalous afterglow” of GRB 050801 recently described by Rykoff et al. (2006). Both bursts show complex behavior in the X-rays as seen with *Swift*-XRT instrument.

Significant “bumps and wiggles” have been seen before in a number of optical afterglows. One of the first well-observed afterglows, GRB 970508 (e.g. Galama et al. 1998) had a light

curve rather similar in shape to GRB 060206, as it brightened by > 1 mag by ~ 2 days after the burst, after which it decayed in a smooth power-law fashion. GRB 000301C exhibited achromatic, short-timescale bump that was difficult to reconcile with the standard relativistic shock model, and which was proposed to be caused by microlensing (Garnavich et al. 2000). GRB 021004 (e.g. Bersier et al. 2003) was not only bumpy, but also showed clear color variations in optical bands (Bersier et al. 2003; Matheson et al. 2003a). GRB 030329 was so bumpy (e.g. Matheson et al. 2003b) that if not for the spectroscopic observations (e.g. Stanek et al. 2003), we would still argue if it showed a “supernova bump” or not. In fact, a significant deviations from a smooth decay have been seen in the light curve of GRB 030329 as late as two months after the burst (so called “jitter event”: Matheson et al. 2003b; Bersier et al. 2006, in preparation). Bumps have also been seen in some previous Swift afterglows (e.g., GRB 050525a: Klotz et al. 2005).

Given the above and the two bursts discussed in this paper, it is becoming clear that the “unusual” or “anomalous” optical afterglows might be more of a norm than an exception. And while “nice and smooth” afterglows have been seen as well (e.g. GRB 990510: Stanek et al. 1999; GRB 020813: Laursen & Stanek 2003; GRB 041006: Stanek et al. 2005) in some well-observed cases, the large number of anomalous optical afterglows can no longer be seen as a small wrinkle on the standard afterglow model. In fact, unless there is sufficient data to suggest otherwise, it would be only prudent to assume that any given afterglow might be anomalous. As a result, some of the often employed procedures, such as deriving the jet opening angle using a broken power-law fit to the optical light curve, in many cases might have a poor statistical significance and be simply not applicable.

Finally, given the totality of the data presented in this paper, we believe that the rise at ~ 3000 sec in the optical for GRB 060206 and the optical bump at ~ 700 sec in GRB 060210 might be due to the turn-on of the external shock—that is, the GRB jet has swept up enough circumstellar/interstellar gas and the magnetic field has developed enough so the standard afterglow has turned-on and it starts to dominate the light in both X-rays and optical. If that is indeed the case, the existence and timing of such features could provide valuable additional information about the energy of the GRB jet and the density of the circumburst medium it is plowing into. This idea is discussed in more detail by Rykoff et al. (2006), when describing the “anomalous afterglow” of GRB 050801.

We thank the *Swift* team, Scott Barthelmy, and the GRB Coordinates Network (GCN) for the quick turnaround in providing precise GRB positions to the astronomical community, and we thank all the observers who provided their data and analysis through the GCN. We thank Weidong Li for useful comments and for providing us with his calibration data for the GRB 060210. We also thank the anonymous referee for useful comments. We also thank

the participants of the morning astro-ph/coffee discussion at the Ohio State University for useful input.

REFERENCES

- Adelman-McCarthy J. K., et al. 2006, ApJS, 162, 38
- Alard, C. 2000, A&AS, 144, 363
- Arnaud, K.A., 1996, ASP Conf. Ser. 101: Astronomical Data Analysis Software and Systems V, ed. Jacoby G. & Barnes J., 17
- Beardmore, A., et al. 2006a, GCN 4724
- Beardmore, A., et al. 2006b, GCN 4733
- Bersier, D., et al. 2003, ApJ, 584, L43
- Beuermann, K., et al. 1999, A&A, 352, 26
- Cool, R. J., et al. 2006, GCN 4695
- Cucchiara, A., et al. 2006, GCN 4729
- Dai, X., & Stanek, K. Z. 2006, GCN 5147
- Falcone, A. D., et al. 2006, ApJ, in press (astro-ph/0512615)
- Fox, D. B., & Cenko, S. B. 2006, GCN 4723
- Fynbo, J. P. U, et al. 2006a, GCN 4683
- Fynbo, J. P. U, et al. 2006b, GCN 4692
- Galama, R. J., et al. 1998, ApJ, 497, L13
- Garnavich, P. M., Loeb, A., & Stanek, K. Z. 2000, ApJ, 544, L11
- Gehrels, N., et al. 2004, ApJ, 611, 1005
- Greco, G., et al. 2006, GCN 4732
- Guidorzi, C., et al. 2006, GCN 4693
- Klotz, A., et al. 2005, A&A, 439, L35

- LaCluyze, A., et al. 2006, GCN 4750
- Laursen, L. T. & Stanek, K. Z., 2003, ApJ, 597, L107
- Li, W. 2006a, GCN 4725
- Li, W. 2006b, GCN 4727
- Lupton, R. 2005
(<http://www.sdss.org/dr4/algorithms/sdssUBVRITransform.htm>)
- Matheson, T., et al. 2003a, ApJ, 582, L5
- Matheson, T., et al. 2003b, ApJ, 599, 394
- Monet, D. G., et al. 2003, AJ, 125, 984
- Morris, D. C., et al. 2006a, GCN 4682
- Morris, D. C., et al. 2006b, GCN 4764
- Nousek, J. A., et al. 2006, ApJ, in press (astro-ph/0508332)
- Perna, R., Armitage, P. J., & Zhang, B. 2006, ApJ, 636, L29
- Piran, T. 2005, RvMP, 76, 1143
- Reichart, D., et al. 2006, GCN 4768
- Rhoads, J. E. 1999, ApJ, 525, 737
- Rykoff, E. S., et al. 2006, ApJ, 638, 5
- Stanek, K. Z., et al. 1999, ApJ, 522, L39
- Stanek, K. Z., et al. 2001, ApJ, 563, 592
- Stanek, K. Z., et al. 2003, ApJ, 591, L17
- Stanek, K. Z., et al. 2005, ApJ, 626, L5
- Wozniak, P. R., et al. 2006a, GCN 4687
- Wozniak, P. R., et al. 2006b, ApJ, 642, L99
- Zhang, B., et al. 2006, ApJ, 642, 354

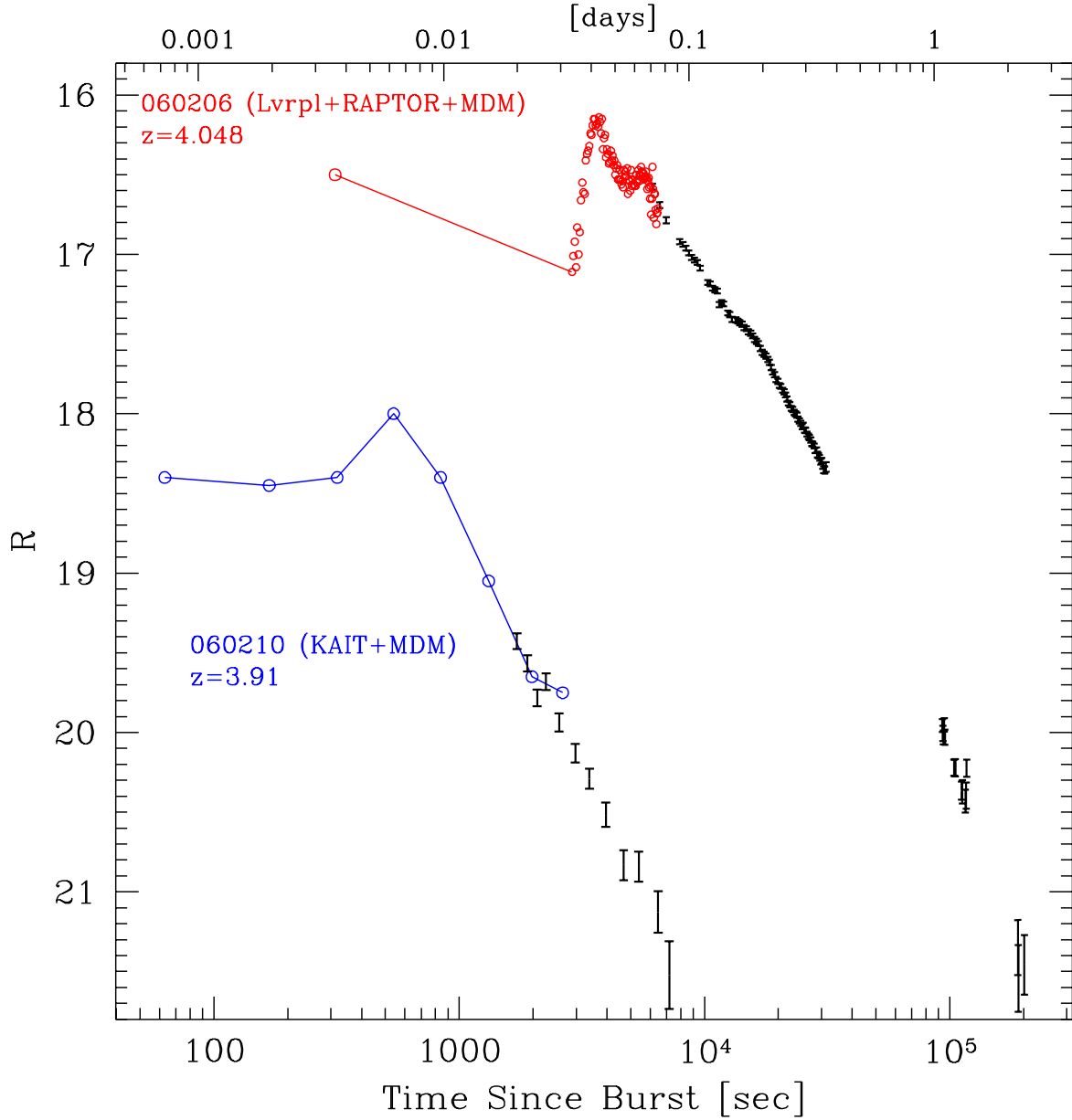


Fig. 1.— R -band light curves of two $z \sim 4$ afterglows, GRB 060206 and 060210. Our data are shown with the error bars, while the data adopted from the literature (GRB 060206: Guidorzi et al. 2006, Wozniak et al. 2006b; GRB 060210: Li et al. 2006b) are shown with the open points, connected together for clarity.

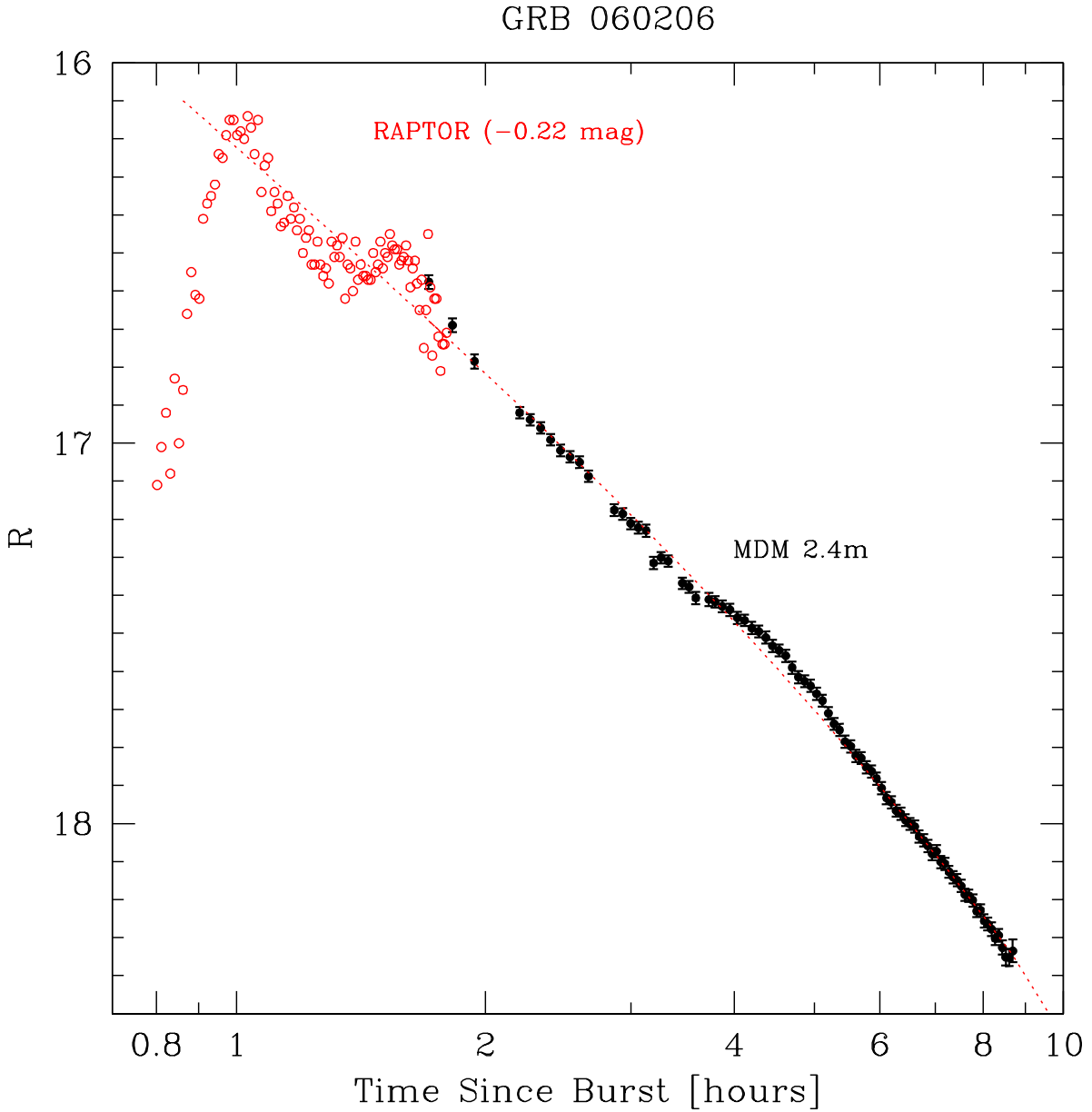


Fig. 2.— R -band light curve of the optical afterglow of GRB 060206 during 0.8 – 8.7 hours after the burst. RAPTOR data (Wozniak et al. 2006b) are shown with open points, shifted by -0.22 mag to match to our data, which are shown as filled points with errorbars. A broken power-law fit to all our R -band data is shown with the dotted line.

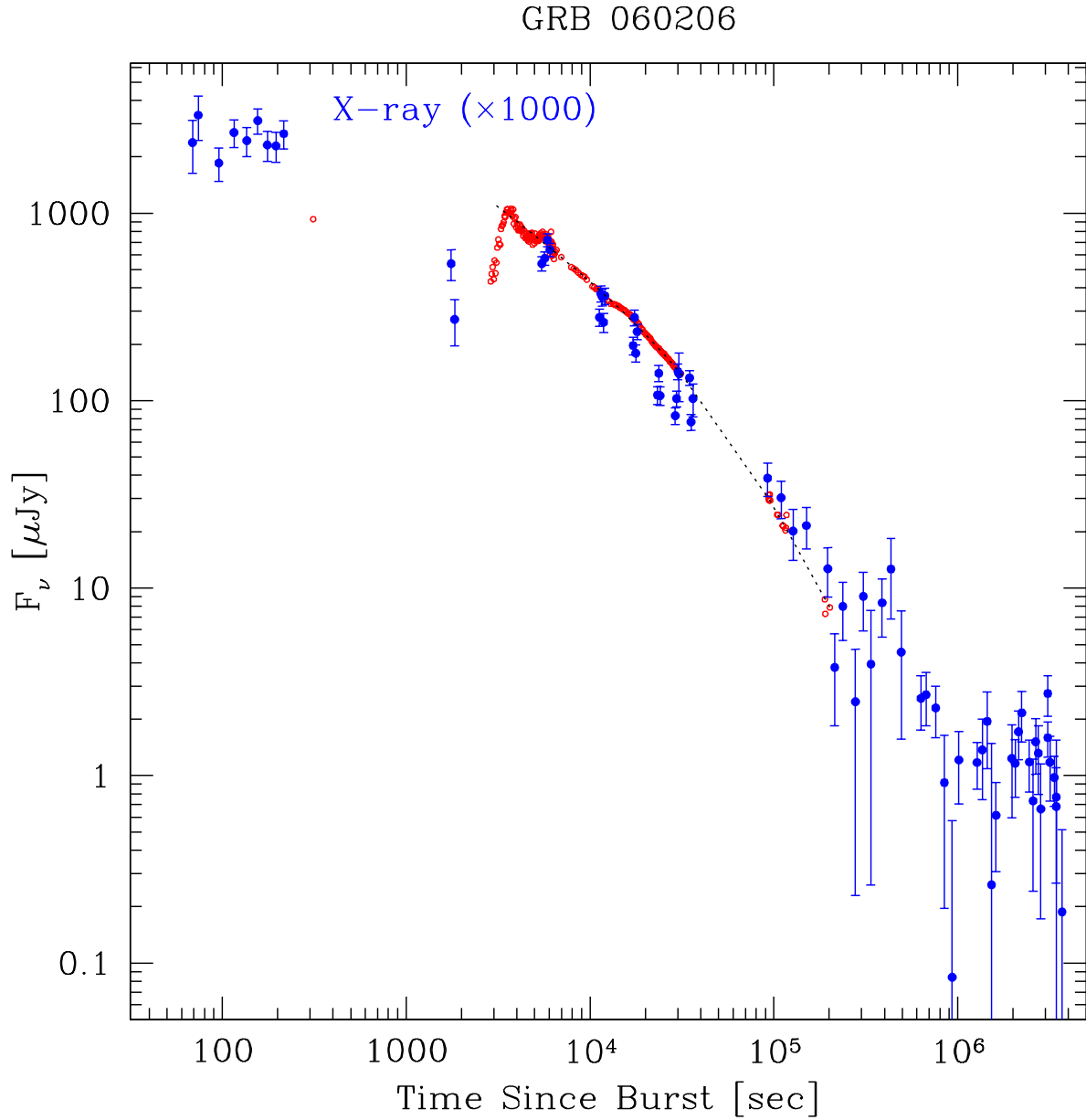


Fig. 3.— Comparison of the R -band (open points) to X-ray light curve (filled points with error bars) for the GRB060206. To better compare to the optical flux, the F_ν for the *Swift* X-ray light curve has been multiplied by a factor of 1000. For the optical data, with the dotted line we show the broken power-law fit described in the text.

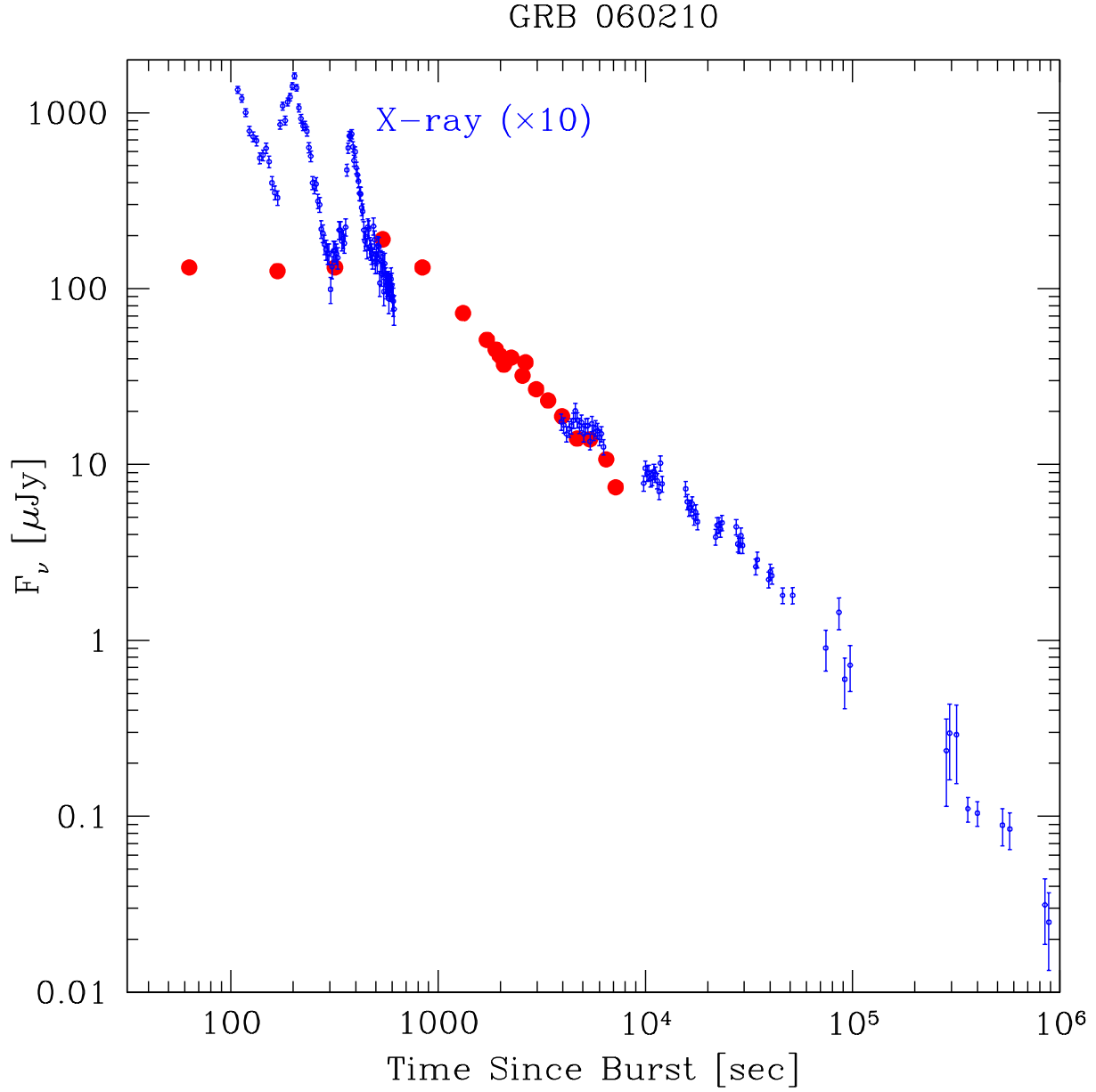


Fig. 4.— Comparison of the R -band data (filled points) to X-ray light curve (error bars) for the GRB060210. To better compare to the optical flux, the F_ν for the *Swift* X-ray light curve has been multiplied by a factor of 10.

Table 1. *R*-BAND LIGHT CURVE FOR GRB 060206

Time [<i>days</i>]	<i>R</i>	σ_R
0.0712	16.576	0.018
0.0760	16.690	0.018
0.0809	16.785	0.019
0.0917	16.920	0.015
0.0944	16.938	0.015
0.0972	16.960	0.015
0.1000	16.991	0.015
0.1027	17.019	0.015
0.1055	17.036	0.015
0.1083	17.050	0.015
0.1110	17.087	0.015
0.1193	17.176	0.016
0.1221	17.186	0.015
0.1249	17.211	0.015
0.1276	17.222	0.016
0.1304	17.230	0.016
0.1332	17.315	0.016
0.1359	17.301	0.015
0.1387	17.310	0.015
0.1442	17.368	0.015
0.1470	17.378	0.016
0.1498	17.407	0.016
0.1553	17.411	0.017
0.1581	17.417	0.015
0.1612	17.429	0.016
0.1646	17.438	0.016
0.1681	17.459	0.016
0.1715	17.466	0.015
0.1750	17.486	0.016
0.1785	17.495	0.016
0.1819	17.511	0.016
0.1854	17.533	0.016
0.1889	17.545	0.016
0.1923	17.559	0.016
0.1958	17.590	0.016
0.1992	17.615	0.016

Table 1—Continued

Time [<i>days</i>]	<i>R</i>	σ_R
0.2027	17.626	0.016
0.2062	17.638	0.016
0.2096	17.659	0.016
0.2131	17.677	0.016
0.2165	17.710	0.016
0.2200	17.738	0.016
0.2235	17.754	0.016
0.2269	17.785	0.016
0.2304	17.797	0.016
0.2339	17.822	0.016
0.2373	17.828	0.016
0.2408	17.852	0.016
0.2442	17.863	0.016
0.2477	17.882	0.016
0.2512	17.907	0.016
0.2546	17.933	0.016
0.2581	17.944	0.016
0.2615	17.966	0.016
0.2650	17.974	0.016
0.2684	17.991	0.016
0.2719	18.001	0.016
0.2754	18.008	0.016
0.2789	18.034	0.016
0.2823	18.044	0.016
0.2858	18.059	0.016
0.2892	18.080	0.016
0.2927	18.073	0.016
0.2962	18.101	0.016
0.2996	18.106	0.016
0.3031	18.127	0.016
0.3065	18.141	0.016
0.3100	18.149	0.016
0.3135	18.164	0.016
0.3169	18.187	0.016
0.3204	18.190	0.016
0.3238	18.202	0.016

Table 1—Continued

Time [<i>days</i>]	R	σ_R
0.3273	18.230	0.016
0.3308	18.228	0.016
0.3342	18.256	0.017
0.3377	18.264	0.017
0.3411	18.278	0.018
0.3446	18.302	0.018
0.3481	18.294	0.017
0.3515	18.326	0.019
0.3550	18.351	0.022
0.3585	18.353	0.022
0.3619	18.335	0.030
1.0802	19.957	0.041
1.0844	20.006	0.048
1.0910	20.032	0.043
1.0993	19.952	0.042
1.1076	20.030	0.047
1.2053	20.221	0.052
1.2137	20.222	0.054
1.2220	20.222	0.054
1.2939	20.364	0.057
1.3023	20.373	0.073
1.3407	20.431	0.072
1.3490	20.397	0.082
1.3556	20.224	0.055
2.1932	21.350	0.173
2.2033	21.543	0.209
2.3331	21.458	0.187

Note. — Table 1 is available in its entirety in the electronic version of the Journal. A portion is shown here for guidance regarding its form and content.

Table 2. *R*-BAND LIGHT CURVE FOR GRB 060210

Time [<i>days</i>]	<i>R</i>	σ_R
0.0199	19.427	0.050
0.0220	19.566	0.051
0.0240	19.783	0.053
0.0261	19.681	0.052
0.0296	19.938	0.057
0.0344	20.130	0.059
0.0393	20.291	0.063
0.0459	20.516	0.076
0.0542	20.833	0.094
0.0625	20.842	0.093
0.0749	21.127	0.130
0.0832	21.523	0.212

Note. — Table 2 is available in its entirety in the electronic version of the Journal. A portion is shown here for guidance regarding its form and content.